Contract No. and Disclaimer:

This manuscript has been authored by Savannah River Nuclear Solutions, LLC under Contract No. DE-AC09-08SR22470 with the U.S. Department of Energy. The United States Government retains and the publisher, by accepting this article for publication, acknowledges that the United States Government retains a non-exclusive, paid-up, irrevocable, worldwide license to publish or reproduce the published form of this work, or allow others to do so, for United States Government purposes.

Testing of 304L Stainless Steel in Nitric Acid Environments With Fluorides and Chlorides

J. I. Mickalonis

Savannah River National Laboratory
Materials Science and Technology

Abstract

Impure radioactive material processed in nitric acid solutions resulted in the presence of chlorides in a dissolver fabricated from 304L stainless steel. An experimental program was conducted to study the effects of chloride in nitric acid/fluoride solutions on the corrosion of 304L stainless steel. The test variables included temperature (80, 95, and 110 °C) and the concentrations of nitric acid (6, 12, and 14 M), fluoride (0.01, 0.1, and 0.2 M) and chloride (100, 350, 1000, and 2000 ppm). The impact of welding was also investigated. Results showed that the chloride concentration alone was not a dominant variable affecting the corrosion, but rather the interaction of chloride with fluoride significantly affected corrosion.

Keywords: Stainless steel, nitric acid, chloride corrosion

Introduction

A traditional method of processing radioactive material involves dissolution in nitric acid solutions containing fluorides. The addition of chloride ions resulting from an impurity complicates the corrosion with expectations of increasing the corrosion rate for 304L stainless steel (304LSS), which is the material of construction for the processing vessels. Both chloride and fluoride ions alone are known to impact the corrosion resistance of 304LS in nitric acid based solutions. Numerous studies have been performed on the effect of these ions individually on the corrosion resistance, but minimal data are available when both species are present.

Nitric acid with fluoride is typically used for dissolution of nuclear materials. As exposure time increases the corrosion behavior progresses from general to intergranular attack (IGA). Grain dropping can occur the most extreme conditions. The degree of attack is also dependent on the concentration of these constituents, temperature, as well as vessel design. The corrosion of stainless steel in nitric acid containing chlorides is a complex interaction of pH, nitrate and

chloride concentrations, time under and temperature. This complexity is shown in part by the maximum degradation of stainless steel occurring at intermediate nitric acid concentrations. If the steel is not immune to the chloride, corrosion generally occurs by pitting.

An experimental program to evaluate the impact of chloride on dissolver corrosion in a nitric acid/fluoride processing solution was developed. The experimental matrix was based on a statistical design to minimize the number of tests and to develop a simple model for predicting corrosion rate. The test variables included temperature, concentrations of nitric acid, fluorides and chlorides, and the presence of a weld. The ranges were chosen to bracket probable process conditions for the dissolver.

Background

The corrosion of 304L stainless steel has not been extensively studied in solutions containing nitric acid, fluoride and chlorides. The most work appears to have been done by the Russians [1,2]. In one case where the chloride was the principle constituent (1N), the addition of fluoride to a chloride/nitrate solution was found to delay pitting due to film formation on the stainless steel [1]. An inhibitive effect for stainless steels was also found for chloride (5,000 ppm) in nitric acid (10M)/fluoride (0.01/0.1 M) solutions at low temperature (20-50 °C) [2].

Extensive testing has been performed for both nitric acid/fluoride (3-6) and nitric acid/chloride solutions (13-16). The corrosion of stainless steel in nitric acid/fluoride solutions generally increases with increasing concentrations of the solution constituents. Gas containment, corrosion products, and type of exposure can greatly accelerate the corrosion. In nitric acid/chloride solutions, the relationship between solution constituents and corrosion rate is more complicated, being affected by pH, time, temperature, as well as nitrate and chloride concentration.

Nitric acid/fluoride solutions have been used extensively world wide for the dissolution of nuclear materials. Early work performed here at SRS and elsewhere showed that the corrosion of 304L stainless steel greatly increased with temperature, fluoride and nitric acid concentration [3-6]. The corrosion rate is also a function of time and increases during initial immersion [8]. The rate has been reported to reach a constant rate in 11-13 M HNO_3 after extended use (>1000 hours), where intergranular attack has lead to grain separation or dropout [9].

The corrosion rate for the vapor space has been reported to be either greater than or less than the liquid exposure [5,10]. This difference appears to be associated with time; short-term test showing vapor space corrosion to be less aggressive. For solutions with 10-13M HNO_3 and 0.04-0.33M HF, which were used to dissolve thorium fuels, the corrosion rate for a batch dissolver operating at 110-115 °C had solution corrosion rates of 25-30 mils per year (mpy) and vapor rates of 40-55 mpy. These rates are lower than for the HB-Line dissolver because thorium complexes the fluoride.

In the vapor space, a thin film of condensate forms on the surface of the stainless steel. This condensate dramatically increases the corrosion rate over time for several reasons. First, the surface area/volume ratio is very large which allows a concentration of oxidizing corrosion products and the access of nitric oxide. Nitric oxide reacts to form nitrous acid which is the

reductant in the corrosion reaction. A ready supply of this species thereby drives the corrosion reaction. Once the corrosion becomes IGA, the penetrations allow for further concentration of the oxidizer.

Welding also impacts the corrosion rate and process of 304L stainless steel in these solutions. Numerous authors have shown that the heat affected zone (HAZ) is attacked intergranularly, which can be associated with either the formation of carbides or impurity segregation that occurs during welding [3-6,11,12]. This can lead to grain drop out and significant ditching. If rates are high enough failure can occur at this location.

In nitric acid/chloride solutions, the corrosion rate as a function of nitric acid concentrations increases to intermediate acid concentrations then decreases with further increases in acid concentration. Kolman et al. investigated extensively the corrosion of 304L stainless in nitric acid/chloride solutions [13]. Corrosion in these solutions was found to be autocatalytic such that self-passivation occurred and caused a change in corrosion rate by orders of magnitude. The time to self-passivation decreased with chloride concentration and surface area/volume ratio. Minimum times for self-passivation were found at an intermediate range of nitric acid concentration. In this range, the maximum susceptibility to pitting was also found.

Similar findings by Petit et al. showed that chloride ions were more effective in less oxidizing solutions, i.e., those with lower nitric acid molarity [16]. Increasing chloride concentrations shifted open-circuit potentials to more active values and reduced the passivity plateau. Increasing nitric acid concentrations also reduced the passivity plateau but shifted the open-circuit potential to more active values. Passive ranges for 304 stainless steel were 0.1-1.0 N HNO_3 and Cl<0.2 %. Pitting occured at lower HNO_3 concentrations and higher Cl, while at HNO_3 concentrations greater than 1.5M intergranular corrosion was noted.

One factor not accounted for in previous testing was the change in the state of chloride in nitric acid solutions. As discussed by Pierce and coworkers, the chloride forms a nitrosyl chloride, which is a soluble gas, at limiting conditions of concentration [15]. Above a nitric acid concentration of 6.5M, the nitrosyl chloride (ClNO) forms. The probable reaction in these solutions is

$$3\ HCl + HNO_3 \rightarrow ClNO + Cl_2 + 2H_2O$$

The formation of nitrosyl chloride would effectively remove the ionic chloride. The solution corrosiveness should decrease if the nitrosyl chloride does not impact stainless steel corrosion. No data could be located about this effect although the pure gas is corrosive to stainless steel and is usually stored in nickel or high nickel alloy containers [18,19].

For austenitic stainless steels, the presence of chlorides can lead to stress corrosion cracking (SCC) with 304L being more susceptible due to its low nickel content. In chloride-containing solutions, SCC is also a function of temperature and solution pH. The occurrence of cracking increases with temperature and decreasing pH [14]. These studies were performed in the absence of other anions. A study on inhibitors for SCC has shown that nitrates are inhibitive to SCC in concentrated chloride solutions [23]. The occurrence of SCC in nitric acid solutions with

fluoride and chloride has not been reported. SCC is more prevalent in solutions where the general corrosion rates are low and less likely at higher rates [24].

Experimental Procedure

The test plan for evaluating stainless steel corrosion consisted of performing coupon immersion testing to determine the corrosion rate under different experimental conditions. The testing was conducted following the ASTM standard G31, "Standard Practice for Laboratory Immersion Corrosion Testing of Metals." The test parameters and values are temperature (80, 95, and 110 °C) and concentrations of nitric acid (6, 8, 12, and 14 M), fluoride (0.01, 0.1 and 0.2 M) and chloride (100, 350, 1000, and 2000 ppm). The values were chosen to establish a statistical test matrix that bracketed a target dissolver condition of 12 M nitric acid, 1000 ppm chloride, 0.1 M fluoride, and 95 °C. The matrix of test conditions is shown in the Table 1. Test periods were generally six hours to simulate the dissolution process. Some testing was conducted for up to 17.25 hours. The generated results were analyzed to model the corrosion in the identified parameter space.

Table 1. Matrix of Experimental Conditions

#	HNO_3 (M)	Cl (ppm)	F (M)	Temp (°C)
1	6	100	0.01	110
2	14	100	0.01	80
3	14	100	0.2	110
4	6	100	0.2	80
5	12	1000	0.1	95
6	14	2000	0.01	110
7	6	2000	0.01	80
8	6	2000	0.2	110
9	14	2000	0.2	80
10	12	350	0.1	95
11	8	350	0.1	95

The test cells were 1-L screw-capped jars made of either Teflon or perfluoroalkoxy polymer resin. Coupons were suspended from the caps to inside the jars with Teflon pipe tape. Three coupons were hung both in the vapor space and in the solution. Solution volumes were 500 ml. The surface area/volume ratio for each coupon was approximately 61 cm^2/L and was similar to that calculated for the dissolver containing 15L of solution. For testing at 110 °C, the test cell was wrapped with heating tapes, which provided improved temperature control and monitoring capabilities. Target temperatures were maintained within ± 0.5 °C. The test cell was fitted with a condenser to minimize water loss, which ranged from 20-50 ml. For testing at 80 and 95 °C, water baths were used. In this case the water bath, not the test cell, was fitted with a condenser. The two test set-ups are shown in Figure 1.

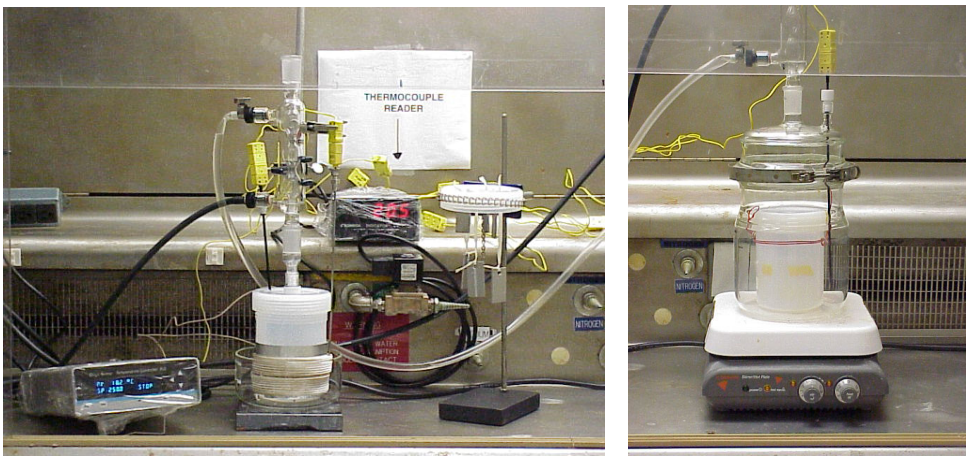

(A) (B)

Figure 1. Experimental Test Set Ups: A) Heating Tape, B) Water Bath

The stainless steel samples were rectangular coupons (2.54 cm wide, 5.08 cm long, 0.32 cm thick) with and without a weld, which was either an autogenous (Series #1 and #2) or butt (Series #3) weld. Samples had a hole in one end for supporting the samples by Teflon® pipe tape. The surfaces were ground on 600-grit silicon carbide paper prior to testing to make the surfaces uniform. The coupons were weighed both before and after testing. When removed from the tests samples were rinsed with water and blown dry prior to weighing.

Test solutions were made up using reagent grade chemicals, nitric acid, sodium chloride and calcium fluoride, and distilled water. Testing was always conducted in fresh solutions to avoid the build up of corrosion products which could lead to higher corrosion rates that might not be representative for the dissolver.

Data Analysis

Corrosion rates were calculated from the weight loss based on the following equation

$$CR = \frac{3.45 \times 10^6 \, W}{A \times T \times D} \qquad \{\text{Equation 1}\}$$

where W is the weight change (grams), A is surface area (cm^2), T is time (hours) and D is density (7.94 g/cm^3). The surface area, 30.6 cm^2, was always taken as that of a new coupon, even for the duplicate tests where the coupons had already been corroded. Corrosion rates were also calculated from the concentrations of iron, nickel, and chromium in the test solutions after an exposure since all corrosion products are in solution.

The testing was executed per a 2^3 factorial design with one center point to provide data for a regression model. Two additional points at 8 and 12M nitric acid with 350 ppm Cl^- were added during test. This level of chloride was tested as a possible limit for the dissolver. A statistical evaluation was conducted resulting in a model being fitted to the data

Results

Chemical Analysis

Solution samples were taken both prior to and after each test condition for some of the tests to evaluated changes in the aggressive anions, chloride and fluoride, and in the stainless steel constituents, chromium, nickel, and iron (Table 2).

The chloride and fluoride concentrations did not change significantly during the course of the test. The fluoride concentration consistently dropped in all test, whereas the chloride concentration either increased or decreased. The nitrate concentration generally increased, which may be associated with a concentration effect. During testing at least 20 ml of solution evaporated. The consistent drop in fluoride is probably associated with the volatization of the fluorides. As can be seen from the table, greater fluoride losses were observed at the higher acid concentrations. This effect was noted previously by other investigators [5].

Table 2. Chemical Analysis Results Of Stainless Steel Corrosion Products And Calculated Corrosion Rates

#	Compositions						Corrosion Rates (mpy)		
	Analytical (ppm)			Calculated (Wt%)			Analytical		Weight loss
	Cr	Fe	Ni	Cr	Fe	Ni	3 coupons	6coupons	Range
1	40	155	18	0.19	0.73	0.08	84	42	60-113
2	45.3	173	20.7	0.19	0.72	0.09	94	47	46-90
3	68.3	263	31.8	0.19	0.72	0.09	143	71	213-980
4	68.3	261	31.6	0.19	0.72	0.09	142	71	25-325
5	145	558	66.1	0.19	0.73	0.09	303	151	91-345
6	93.5	355	43.1	0.19	0.72	0.09	194	97	18-100
7	6.68	26.4	3.22	0.18	0.73	0.09	14	7	4-12
8	740	2850	336	0.19	0.73	0.09	1546	773	134-1768
9	267	1010	120	0.19	0.72	0.09	550	275	62-330
10	183	686	82.7	0.19	0.72	0.09	375	187	64-303
11	230	868	105	0.19	0.72	0.09	474	237	60-300

The calculated compositions are in good agreement with the nominal values for 304L stainless steel. In some cases the percentage is slightly greater than 100% due to rounding. Corrosion rates were calculated using surface areas for three or six coupons. Although only three coupons were immersed in the solutions, the three vapor coupons dripped condensate into the solution. For solution #3 which was run at 110 °C, the analysis had extremely low values for even the three-coupon calculation. The source of this error is not known. In most cases the calculated corrosion rate using the surface area for six coupons fell within the range of values calculated from weight losses.

Corrosion Loss

The corrosion rates for 304L in the different test conditions were calculated from the coupon weight losses for all the series. The average rates varied by approximately two orders of magnitude (for liquid exposure 10-1191 mpy, for vapor exposure 6-419 mpy). For the liquid exposure the lowest and highest values both occurred with 6 M nitric acid and 2000 ppm chloride solutions. The low value was with the low fluoride and temperature and the high value was with high fluoride and high temperature. In Table 3, the range of corrosion rates and average values for both the liquid and vapor exposure are given for each test condition. As can be seen by a comparison of the data, the corrosion rates in the liquid were greater than those in the vapor. The ratio of the rates varies from 1.2 to 5.5.

The test conditions can be divided into three corrosion categories by the corrosion rate. The corrosion categories and rates (CR) are low with CR<200 mpy, medium with 200 <CR<500 mpy, and high with CR>500 mpy. The low category consists of six conditions with low fluoride or low temperature. The medium category had three conditions with the medium values. The high category had always high fluoride and temperature.

Table 3. Average Corrosion Rates For Test Conditions Based On Weight Losses

Acid (M)	Cl (ppm)	F (M)	Temp (C)	Corrosion Rate (mpy)		
				Range	Average	
					Liquid	Vapor
6	100	0.01	110	60-113	88	46
		0.2	80	25-325	190	47
6	2000	0.01	80	4-12	10	6
		0.2	110	134-1768	1191	217
8	350	0.1	95	60-300	278	80
12	350	0.1	95	64-303	280	128
	1000	0.1	95	91-345	224	163
14	100	0.01	80	46-90	65	54
		0.2	110	213-980	676	419
	2000	0.01	105	18-100	75	52
		0.2	80	62-330	193	131

Morphological Analysis

The corrosion morphology of the coupons varied considerably depending on the test condition and the exposure. The heavily corroded coupons had a dull, rough surface, whereas a metallic sheen was still apparent on the coupons with the lowest corrosion rate. The liquid-exposed coupons always had a more degraded surface than the vapor-exposed coupons, although the vapor coupons had spots where the corrosion appeared more aggressive than the surrounding metal. Corrosion also highlighted the presence of the weld except for the coupons with the lowest corrosion rate (~10 mpy).

The corrosion morphology of the coupons can be discussed with reference to the corrosion rate categories. In the low category the coupons still clearly had the grinding marks, although the surface was degraded or roughened. Hemispherical pits were generally not observed but rather

pitting initiated at surface imperfections. These pits had an angular appearance on the pit perimeter. In the high-chloride solution of this category, very small hemispherical pits were found.

In the medium category, small shallow pits covered the surface. Some of these pits were also associated with surface imperfections. Ghost of the grinding marks remained, which resulted from the corrosion of the initial peaks and valleys.

The high category, which had two test conditions, had two different corrosion morphologies. The first was similar to those for the medium category and occurred with a low chloride but high acid concentration. The second morphology occurred for only the liquid exposure with the low acid and high chloride concentration. The coupons were characteristically different from all the others. The surface was extremely roughened and showed the initial onset of intergranular attack (IGA) where grain boundaries started to appear differentiated. Shallow pits were observed, which were attributed to the high corrosion rate. The vapor-exposed coupons for this test condition had surface morphologies similar to the medium category. Figure 2 shows the morphology for both the vapor and liquid exposures.

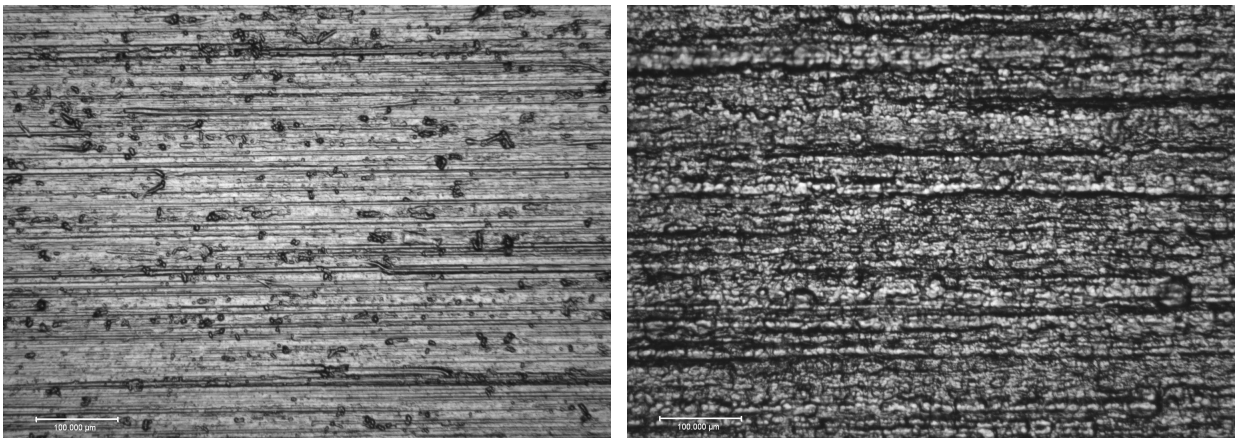

(A) (B)

Figure 2. Micrographs of 304 L Stainless Steel Exposed to 6M HNO_3, 2000 ppm Cl^-, 0.2M F^- at 105 °C: (A) Vapor exposure, (B) Liquid exposure

Corrosion also occurred at impurities or inclusions, which were aligned along the rolling direction. This phenomenon was noted on coupons with the rolling direction perpendicular to the direction of grinding. Most coupons had these two directions parallel. Pitting was found aligned in the rolling direction, as well as more corrosion at the grain boundary interfaces where troughs developed. Figure 3 shows this corrosion along the rolling direction for a coupon exposed to the 12 M HNO3, 1000 ppm Cl, 0.1M F at 95 °C.

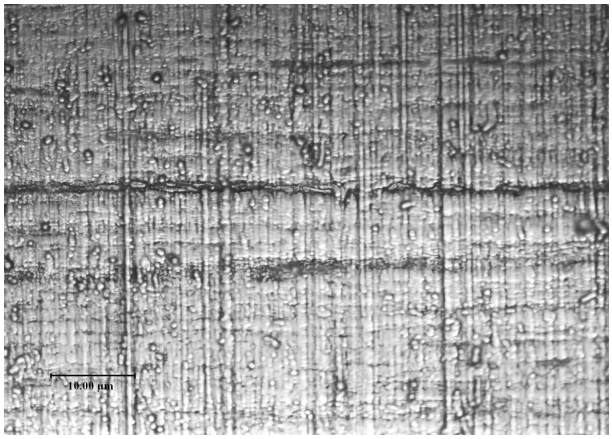

Figure 3. Micrographs of 304 L Stainless Steel Immersed in 12 M HNO_3, 1000 ppm Cl^-, 0.01M F^- at 95 °C

For the welded coupons, the base metals were similar to the descriptions given above. In the heat affected zones (HAZ) the corrosion appeared to be more aggressive than the remaining coupon. Some ditching was observed in this region, with grain boundaries being highlighted. Pitting or corrosion of the interdendritic regions of the adjacent weld was also observed. Figure 4 shows the typical morphology observed in most welded coupons.

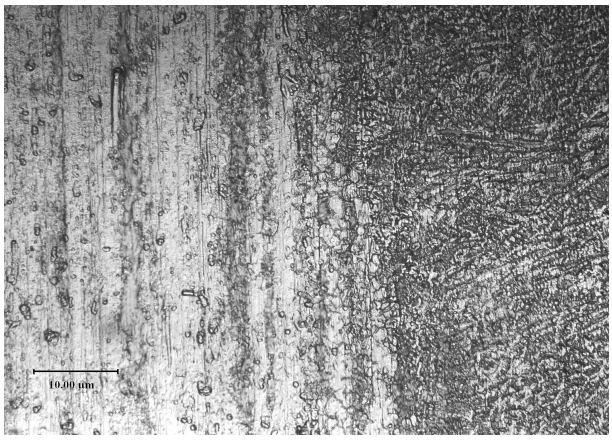

| Base Metal |HAZ | Weld Metal |

Figure 4. Micrographs of 304 L Stainless Steel Exposed to the Vapors from 6M HNO_3, 2000 ppm Cl^-, 0.2M F^- at 110 °C

Statistical Analysis

The statistical analysis was performed using either the mean value or the natural logarithm. Two six-hour tests were performed on the same coupon at the same test condition. For the target condition (12 M HNO_3, 0.1 M F^-, 1000 ppm Cl^- at 95 °C), three six-hour test were run for a total time of 18 hours. The tests were structured this way to evaluate changes in the corrosion rate

with a corroded surface. The rates were found not to change significantly. The observed changes in rate, an increase or a decrease, were not consistent for the various test conditions. The corrosion rates of the welded and regular coupons did not differ significantly (at 5% significance level) using several different bases. The difference was evaluated for the complete set of data, for liquid and vapor exposures separately and for each test condition. Both the mean difference and natural logarithm of the mean were used. Initially a difference in rate was expected since the corrosion of the HAZ was expected to be greater. The lack of observed ditching on the welded coupons was probably associated with the short total time of the testing (usually 12 hours).

The significant variables affecting the corrosion rate were evaluated including temperature and the concentrations of fluoride, chloride and nitric acid as well as any interactions between these variables. The temperature was the most important variable.

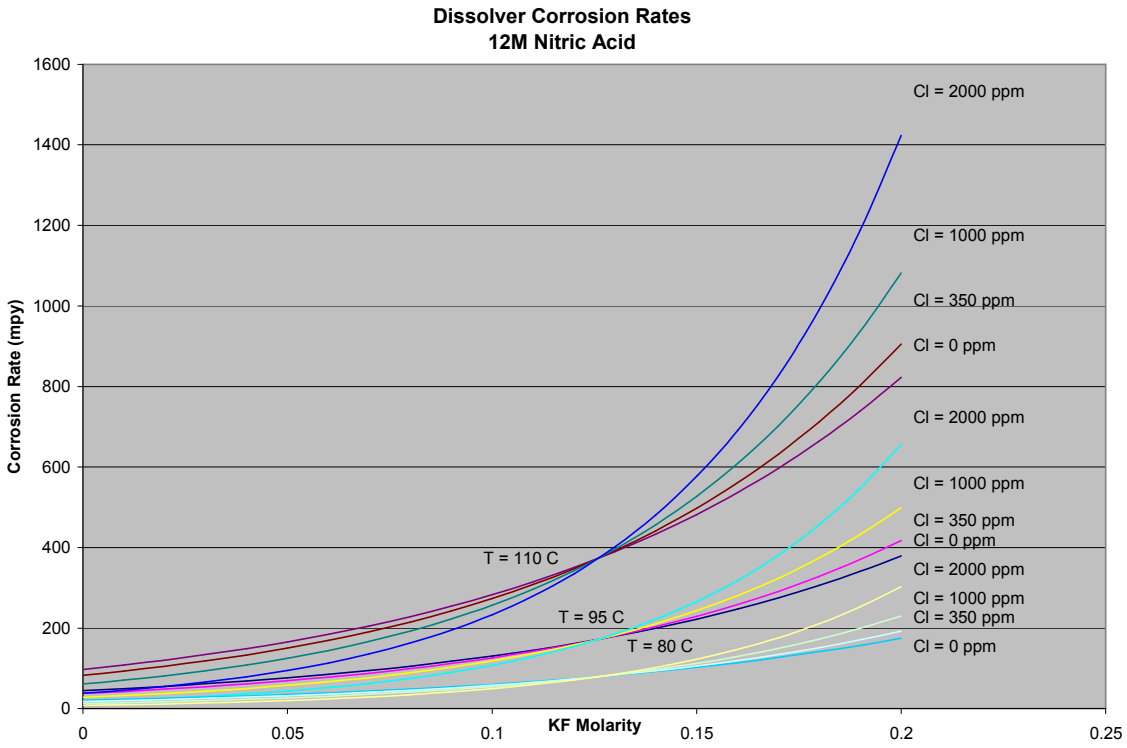

Figure 5. Graphical Presentation of Equation 2, the Corrosion Rate Model For 304L Stainless Steel Immersed in Nitric Acid Solutions Containing Chloride and Fluoride

Some interactions were also significant. For the liquid exposure, the acid/fluoride and chloride/fluoride interactions were important, whereas for the vapor only the chloride/fluoride interaction was significant. With all the data analyzed together, temperature and fluoride concentration were the significant primary variables. Acid and chloride concentrations were not significant although the interactions of these variables with fluoride were important. The models differed slightly for the liquid and vapor exposure. The liquid model predicted 90 % of the data and the vapor model approximately 80%. The model for the liquid exposure is

$$CR = Exp(-1.0726 + 10.4696\ F + 0.0516\ T - 0.9106\ (A-10.1176)(F-0.1259) + 0.0037\ (C-958.824)(F-0.1259)), \quad \text{\{Equation 2\}}$$

where CR is corrosion rate (mpy), F is fluoride concentration (M), T is temperature (°C), A is acid concentration (M), and C is chloride concentration (ppm). For a graphical presentation of this equation shown in Figure 5, the corrosion rate was plotted for a constant nitric acid concentration of 12M, the target value, as a function of fluoride concentration. The different sets of lines are for different temperatures. Within each temperature, the lines are for different chloride concentrations. This graph clearly shows that the corrosion rate increases with increasing temperature and concentrations of fluoride and chloride.

Discussion

The importance of the chloride concentration on the corrosion of stainless steel is impacted by the change in chloride species with nitric acid concentration. The measured chloride concentrations from pre- and post-test solutions given in Table 2 show that the ionic chloride concentration changes with the nitric acid concentration. As Pierce has shown, the chloride reacts with the nitric acid to form nitrosyl chloride[17]. The reaction becomes significant above an acid concentration of 6.5 M. For the 6 M HNO_3 solutions with a make up quantity of 2000 ppm, approximately the same quantity of ionic chloride was found in solution. For the 12 and 14M HNO_3 solutions, the ionic chloride concentration was in a range of 300-450 ppm. The large quantity of nitrate in these solutions may be impacting the chloride measurement since the solutions with 100 ppm chloride were also measured with values near and within this range. This effect is currently being investigated.

From the testing and statistical analysis, chloride concentration was not found to be a significant variable influencing corrosion. The primary variables of importance were the temperature and fluoride concentration. Both acid and chloride concentration were important for their interactions with the fluoride concentration. For the chloride concentration, this effect was shown graphically in Figure 5 where the interaction becomes more important as the fluoride concentration increases.

From the model shown in Figure 5, at fluoride concentrations less than 0.125M the corrosion rate drops with increasing chloride concentration which is similar for 6 and 14M nitric acid solutions. A competitive effect between the two aggressive anions may be occurring at these low fluoride concentrations. This inhibitive effect had also been noted by the Russian investigators testing in 10M nitric acid with 0.01 and 0.1M fluoride and 5000 ppm chloride [2]. The paper was unclear whether this effect was observed at 0.01 or 0.1 M fluoride.

The total time tested is short in comparison to the extended exposure times for a typical dissolver. Rates are expected to increase over extended operation as the corrosion morphology and process changes. With the onset of IGA, the localized environments within the grain boundary grooves will become more oxidizing due to the increasing presence of corrosion products, especially chromium ions. Also, the inhibitive effect of chlorides at low fluoride concentrations (< 0.12 M) cannot be assumed since a change in mechanism has occurred.

The corrosion processes that were noted during these tests included general corrosion, pitting, and IGA. General corrosion and IGA also occurred with just nitric acid/fluoride solutions. General corrosion with or without chloride is at a significant rate and leads to wall thinning. If solutions become more oxidizing, then the onset of IGA can be expected. These oxidizing conditions can develop from increased corrosion product concentration, crevice formation, or increasing nitric acid concentration.

Some of the vapor coupons showed the initiation of IGA from the thin liquid layers that formed from the condensate, which can be more oxidizing than bulk liquid conditions. Vapor corrosion rates for nitric acid/fluoride environments have been reported to be greater than liquid exposures for extended hours of continuous operation at temperature where IGA eventually lead to grain dropping [5,6,16]. Grain dropping will lead to large corrosion rates.

In this testing which simulated dissolver operation, the vapor corrosion rates were found to be lower. The presence of IGA on these coupons indicates that for the dissolvers vapor space corrosion would initially be low. After extended use, the IGA would be expected to increase and the vapor corrosion rate would be expected to increase over time. This corrosion would be expected in both the dissolver and hot sections of the off gas system.

The pitting that occurred during this testing was always found to be shallow (<0.0005 in). The high corrosion rates of these solutions may not provide conditions for high pitting rates to develop and lead to a leak prior to significant use of the dissolver vessel.

Conclusions

The corrosion of 304L stainless steel in nitric acid solutions containing chlorides and fluorides changed significantly depending on the concentrations of the solution constituents and temperature. The primary variables affecting the corrosion rate were temperature and fluoride concentration. If the fluoride concentration and temperature are low, corrosion rates are generally less than <200 mpy where a general corrosion mechanism occurs with minimal pitting. At high values for fluoride and temperature, corrosion rates increased dramatically, which can lead to a faster onset of IGA.

Chloride concentration was not a dominant variable affecting the corrosion, but rather the interaction of chloride with fluoride; that is the effect of chloride is dependent on fluoride concentration. At low values of fluoride the chloride has an inhibitive effect, while at higher levels the chloride accelerates the corrosion. The effect of chloride is further complicated by the

formation of nitrosyl chloride which reduces the ionic concentration. The effect of nitrosyl chloride on the corrosion was not studied.

Acknowledgements

The author gratefully acknowledges K. R. Hicks for her role in performing the majority of the experimental work, V. Timmerman and K. Kalbaugh for their assistance with additional experimental work, C. Sexton for making the glassware and R. Pierce for his advice and observations during the testing.

References

1. V. S. Kuzub and V. S. Novitskii, "Effect of F, $H_2PO_4^-$ and SO_4^{--} ON Pitting Corrosion Of Steel 1Kh18N10T In Chloride-Nitrate Solutions," Zaschita Metallov, 12 (1), 52-55, 1976.

2. E. V. Konstantinova and V. I. Lomovtsev, "Corrosion of Low-Nickel and Nickel Free Stainless Steels In Concentrated Nitric Acid With Hydrofluoric Acid or Chloride Ions," Zaschita Metallov, 19(6), 933-934, 1983.

3. R. S. Ondrejcin and B. D. McLaughlin, "Corrosion of High Ni-Cr Alloys and Type 304L Stainless Steel in HNO_3-HF," DP-1550, April 1980.

4. P. M. Kranzlein et al.,"Corrosion of Stainless Steel in HNO_3-HF Solutions," DP-486, July 1960.

5. H. S. Cole, "Corrosion of Austentic Stainless Steel Alloys Due to HNO_3-HF Mixtures," ICP-1036, October 1974.

6. M. W. Wilding and B. E. Paige, "Survey on Corrosion of Metals and Alloys in Solutions Containing Nitric Acid," ICP-1107, December 1976.

7. J. I. Mickalonis, "Corrosion Loss Analysis of HB-Line Dissolvers (U)," WSRC-TR-2005-00082, February 2005.

8. J. E. Truman, "Factors Affecting the Testing o Stainless Steels in Boiling Concentrated Nitric Acid," J. Appl. Chem., 4 (5), 273-283, 1954.

9. M. Mayuzumi et al., "Effects of Cold Work, Sensitization Treatment and the Combination on Corrosion Behavior of Stainless Steel in Nitric Acid," Corrosion, 54(4), 271-280, 1998.

10. F. Balbaud et al., "Mechanism of Corrosion of AISI 304L SS in the Presence of Nitric Acid Condensates," Corr Sci, 42, 1685-1707, 2000

11. J. S. Armijo, "Intergranular Corrosion of Nonsensitized Austenitic Stainless Steels," Corrosion, (1), 24-30, 1968.

12. M. Mayuzumi et al., "Synergistic Effect of Impurities on the Corrosion Behavior of Fe-18%Cr-14Ni Alloys in Concentrated Nitric Acid," 59 (4), 345-349, 2003.

13. D. G. Kolman et al., "Corrosion of 304 Stainless Steel Exposed to Nitric Acid-Chloride Environments," Corr Sci, 39(12), 2067-2093, 1997.

14. J. E. Truman, "The Influence of Chloride Content, pH and Temperature of Test Solution on the Occurrence of Stress Corrosion Cracking With Austenitic Stainless Steel," Corr Sci, 17(), 737-746, 1977.

15. H. P. Leckie and H. H. Uhlig, "Environmental Factors Affecting the Critical Potential for Pitting in 18-8 Stainless Steel," J. Electorchem Soc, 113(12), 1262-67, 1966.

16. M. C. Petit et al., "The Electrochemical Behavior of SS in Hot Nitric Solutions as Related to SCC Phenomenon," Corr Sci, 32(12), 1315-1329, 1991.

17. R. A. Pierce and R. P. Campbell-Kelly, "Engineering-Scale Demonstration For Aqueous Chloride Removal Using Nitrogen Dioxide Gas," WSRC-STI-2006-00366, December 2006.

18. US Patent 3987150, "Production of Ammonium Nitrate.

19. www.specialmetals.com, "High Performance Alloys For Resistance To Aqueous Corrosion" Specialty Metals Company, 2007.

20. W. R. Hinz and J. I. Mickalonis, "HB-Line Dissolver Corrosion Degradation," WSRC-TR-2006-00195, May 2006.

21. P. R. Vormelker, "Analysis of Leaking HB-Line Dissolver Tank, RD-13 (U)," SRT-MTS-2000-40147, October, 20, 2000.

22. S. Y. Lee, "Simulation Analysis for HB-Line Dissolver Mixing," WSRC-TR-2005-00028, November, 2005.

23. M. L. Holzworth and A. E. Seymonds, " ," Corrosion, 25(), 287, 1969.

24. Stress-Corrosion Cracking of Austenitic Chromium-Nickel Stainless Steels, ASTM STP No. 264, American Society For Testing Materials, Philadelpia, PA, 1960.

25. Personal Communication with C. F. Jenkins.